

Development of a Dynamic Fouling Model for a Heat Exchanger

Khayyam Zahid, Rajnikant Patel, Iqbal Mujtaba*

School of Engineering and Informatics, University of Bradford, Bradford, BD7 1DP, UK
 I.M.Mujtaba@bradford.ac.uk

Fouling in heat exchangers (HE) is a major problem in industry and accurate prediction of the onset or degree of fouling would be of a huge benefit to the operators. Modelling of the fouling phenomenon however, remains a challenging field of study. Cleaning of heat exchangers, coupled with the down time, is a financial burden and for industrialized nations and costs can reach to almost 0.25 % of the country's Gross National Product (Pritchard, 1988). This work presents the development of a dynamic fouling model based on experimental data collected using a laboratory concentric tube heat exchanger handling a saline system. Heat transfer coefficients were obtained from first principles as well as from either the Sieder-Tate or Petukhov-Kirillov correlations modified by Gnielinski depending on the flow regime. The outlet temperatures were calculated using the Effectiveness-NTU method. The dynamic fouling factor was based on the Kern and Seaton fouling model and validation was completed by comparing the experimental outlet temperatures with those predicted by the model. The model predicts the outlet temperatures with an average discrepancy of 1.6 °C and 0.4 °C for the cold and hot streams respectively.

1. Introduction

Fouling is a general term used to describe the deposition of foreign matter on a heat transfer surface. The gradual deposition process remains a great concern when considering heat exchanger installation as it can affect both heat transfer and fluid flow. Costs associated with heat exchanger fouling include increased energy consumption, downtime, cleaning, and can also exacerbate problems associated with membranes (Shirazi, 2010). Heat exchanger maintenance costs arise from fouling deposit removal through chemical or mechanical means; as well as the replacement of corroded or plugged equipment. Other costs include increased capital cost due to oversized or redundant equipment and energy wastage due to an increased heat transfer coefficient (Georgiadis et al., 1998). Within the dairy industry, it is estimated that fouling removal via cleaning can account for around 15 % and 80 % of extra production time and costs (Mérian et al., 2012). The simulated temperature profiles can also be used to identify potential weak spots concerning fouling (Jun et al., 2004). An example of non-optimal control implementation involves maintaining a wall temperature that is too high or product flow rate that is too low which can ultimately increase the severity of fouling (Fryer, 1989). Various models have been proposed in an attempt to model and predict fouling behavior (Müller-Steinhagen, 2011) and more recently Arsenyeva (2012). In order to improve model reliability, multiple experiments and simulations have been conducted; nevertheless fouling problems within industry are still not accurately predicted leading to non-optimal fouling mitigation. Recent fouling model developments involve using CFD to predict fouling and are in agreement with previously published experimental results and theoretical models (Haghshenasfard, 2015 and very recently (Pääkkönen, 2016).

The aim of this work is to develop a model for fouling in a heat exchanger which can effectively predict the heat transfer behaviour when a saline fluid is introduced to the system. Discrete rather than dynamic fouling factors are often added to calculate overall heat transfer co-efficient in heat exchangers. This will not be the case in this study as a dynamic fouling factor will be used in order to account for losses in heat transfer efficiency over time. To prove the validity of this model, an experiment has been conducted to verify the model accuracy.

2. Double pipe heat transfer coefficient

The fouling model of a double pipe heat exchanger requires the calculation of four heat transfer coefficients namely that of the inner tube, annulus space, tube wall, and fouling surface. Heated saline water will be carried through the inner tube which will be cooled using water supplied through the annulus. For this reason the annulus space heat transfer coefficient will be modelled as a constant as there is no fouling within the shell and therefore the diameter will remain unchanged. The wall heat transfer coefficient will also be modelled as a constant. The following assumptions are made to reduce system complexity: No condensation; no leakage; no heat loss to environment; and constant tube diameter. The Nusselt number for the inner tube (Nu_{hot}) and annular space (Nu_{cold}) is a function of the Prandtl number (Pr) and Reynolds number. For laminar flow, the Sieder and Tate correlation is used (Sieder et al., 1936).

$$Nu_i = 1.86 \left(\frac{Re_i Pr_i D_{e,i}}{L} \right)^{\frac{1}{3}} \left(\frac{\mu_i}{\mu_{water}} \right) \quad (1)$$

Where L is the tube length and Pr is within 0.48 and 16,700. The value of $\left(\frac{Re_i Pr_i D_{e,i}}{L} \right)^{\frac{1}{3}}$ must also be less than 2. For turbulent flow, the following correlation developed by Petukhov-Kirillov modified by Gnielinski can be used (Gnielinski, 1975).

$$Nu_i = \frac{\left(\frac{f_i}{8} \right) (Re_i - 1000) Pr_i \left(1 + \frac{D_{e,i}}{L} \right)^{\frac{2}{3}}}{1 + 12.7 \left(\frac{f_i}{8} \right)^{0.5} (Pr_i^{2/3} - 1)} \left(\frac{\mu_i}{\mu_{water}} \right)^{0.14} \quad (2)$$

Where f_i is the friction factor calculated using

$$f_i = (0.782 \ln(Re_i) - 1.51)^{-2} \quad (3)$$

The overall clean heat transfer coefficient of the system (U_c) is a function of the inner tube heat transfer coefficient (h_{hot}) annulus space transfer coefficient (h_{cold}) wall thermal conductivity (k_w) and wall thickness, (THK_w) during the first pass of the system.

$$\frac{1}{U_c A} = \frac{1}{h_{hot} A_{f,hot}} + \frac{1}{h_{cold} A_{f,cold}} + \frac{THK_w}{k_w A_{f,w}} \quad (4)$$

The dynamic fouling factor can be thought of as an additional heat resistance layer and given as

$$U_f = \frac{U_c}{1 + U_c R_f} \quad (5)$$

Where R_f will be obtained experimentally in this work.

3. Dynamic fouling factor

In order to accurately model this specific system, the fouling factor R_f must be obtained through experimental means. Examples of fouling factor generic models can be found but are not an all-encompassing solution to obtain a direct relationship between fouling and time as they do not take into account all parameters such as temperature, flow rate etc. for a specific system. For this reason, it is best to obtain a fouling factor through experimental methods.

3.1 Experimental procedure

Prior to system start up, a saline solution was made up using 3 grams of regular table salt per 100 grams of water giving a salt concentration of 30,000 ppm (typical seawater salinity). Initial checks were made to ensure all tubing was connected and the equipment was safe to use. The system was set to run in counter-current operation and the hot fluid temperature was set to 40 °C (313.16 K, typical of last stage temperature of Multistage Flash Desalination process) whilst the cold fluid temperature was set to 20 °C (293.16 K, typical of winter seawater temperature). Both hot and cold fluid flow rates were set to 1 L/min. Figure 1 shows the experimental set-up. The saline fluid was heated in a water bath before being pumped through the double pipe heat exchanger via a flow control valve. A refrigerated circulating bath was used to control the inlet cold water temperature and this was also pumped through the HE via a flow control valve. As the system is closed loop, the system temperature was allowed to stabilise before data logging began. The inlet and outlet temperatures for both streams were monitored and data was sampled every minute for a total duration of 12 h.

3.2 Experimental results

Figures 2 and 3 show a cooling/heating gradient of around 4 °C was observed throughout the duration of the experiment. The 0.5 °C variance in cooling fluid temperature can be accounted for as the system was turned off overnight and restarted in the morning in order to minimize the risk of damage to the system by leaving the system unattended for an extended period of time. Data logging began when the system reached steady state which took around 90 min. The next step in calculating the fouling factor was to observe how the cooling or heating changed over time.



Figure 1: Fouling experiment apparatus

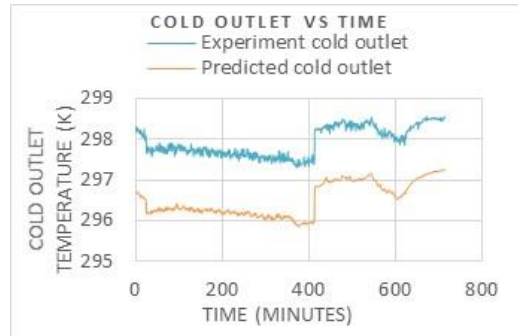


Figure 2: Cold stream outlet temperature (experiment and prediction)

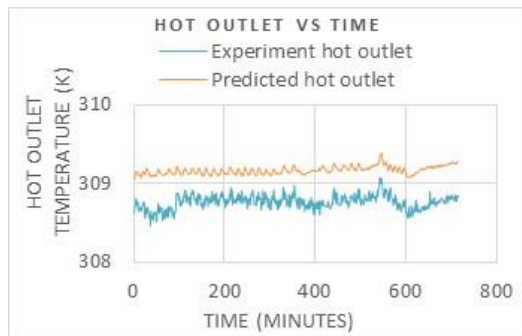


Figure 3: Hot stream outlet temperature (experiment and prediction)

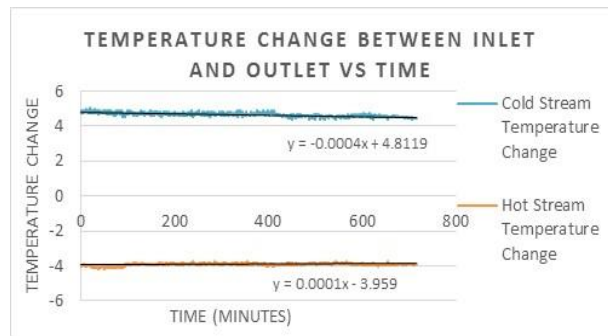


Figure 4: Temperature change between inlet and outlet against time

Figure 4 shows the temperature change over time where the temperature change was calculated using Eq(6). In this time period, the cold stream temperature change decreases over time indicating a lower heat transfer rate. This trend is also observed for the hot stream where the temperature change decreases. The decrease in heat transfer can be explained due to the increase in salt deposit over time which creates a larger heat resistance layer. The calculation of temperature change at time i is given as:

$$T_{change,i} = (T_{out,i} - T_{in,i}) \quad (6)$$

Although Figure 4 establishes that heat transfer decreases over time, the actual rate of heat transfer decay is not established i.e. effect of fouling on temperature change. Figure 5 shows the decay rate of temperature change over time. In order to establish a degeneration rate regarding heat transfer, an average temperature change is calculated by taking the mean of the first 120 values of temperature change and comparing them to the temperature change at the current time. The calculation assumes minimal fouling occurs in the first 120 minutes and therefore baseline temperature change decay is close to 0. Figure 5 shows the average temperature change of the hot stream outlet has increased by around 0.1 °C after 800 min and the average temperature of the cold stream outlet has decreased by around 0.3 °C. The calculation at time i is given as:

$$T_{decay,i} = T_{change,i} - \frac{\sum_{t=0}^{t=120} T_{change,i}}{120} \quad (7)$$

The term $\frac{\sum_{t=0}^{t=120} T_{change,i}}{120}$ can be thought of as the average temperature change when little to no fouling has occurred.

Figure 6 shows the change in efficiency of the heat exchanger over time as a result of fouling. In order to establish the efficiency of the heat exchanger, the following equation is used:

$$HE_{efficiency}(\%) = \frac{T_{decay,hot} + \frac{\sum_{t=0}^{t=120} T_{change,hot}}{120}}{\frac{\sum_{t=0}^{t=120} T_{change,hot}}{120}} \quad (8)$$

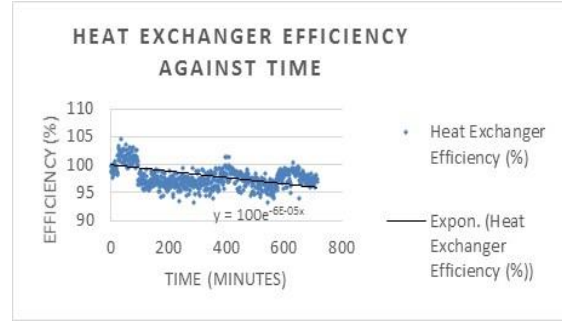
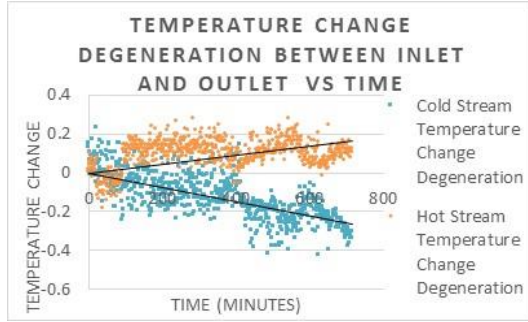


Figure 5: Temperature change degeneration between inlet and outlet against time

Figure 6: Heat exchanger efficiency against time

The term $\frac{T_{decay,i} + \frac{\sum_{t=0}^{t=120} T_{change,i}}{120}}{\frac{\sum_{t=0}^{t=120} T_{change,i}}{120}}$ can be thought of as the heat transfer efficiency of the stream i as the addition of

the decay term considers the effect of fouling. Figure 6 shows that the heat transfer efficiency starts at 100% and decays to around 96 % after 800 minutes.

The clean heat transfer coefficient ($U_{clean}A$) and heat exchanger efficiency ($HE_{efficiency}$) are known. In order to calculate the heat transfer coefficient decay, the following equations are used:

$$U_f A = (U_{clean}A)(HE_{efficiency}) \quad (9)$$

$$(UA)_{decay} = (U_f A) - (U_c A) \quad (10)$$

Figure 7 shows the relationship between UA_{decay} and time. This relationship can be used as the fouling factor (R_f). It can be seen that the heat transfer rate has decreased by $0.6 \frac{W}{m^2K}$ over 700 min. The overall equation for $U_f A$ can be written as:

$$U_f A = U_c A + (0.00000003t^2 - 0.0009t) \quad (11)$$

Although the overall heat transfer equation has been established, it is not in the form of the Kern and Seaton asymptotic model (Kern and Seaton, 1959):

$$R_f = R_f^* \left(1 - e^{-\frac{t}{t_c}} \right) \quad (12)$$

Where R_f is the fouling resistance, R_f^* the asymptotic fouling resistance, t the current time and t_c the residence time. The thickness of the fouling deposit is derived as:

$$THK_f = \frac{-k_f A_{f,f} (UA)_{decay}}{((UA)_{decay} + U_c A) U_c A} \quad (13)$$

Figure 8 shows that the thickness of the fouling deposit increases from 0 to around 0.0002 mm over 700 min which is expected as the flow rates and temperatures were very low. Since $A_{f,f}$ is unknown, $A_{f,w}$ is used in its place as this is a conservative value assuming the fouling deposit area will not become greater than the heat transfer area of the wall. The Kern and Seaton equation can be written as:

$$\frac{THK_f}{k_f A_{f,f}} = R_f^* \left(1 - e^{-\frac{t}{t_c}} \right) \quad (14)$$

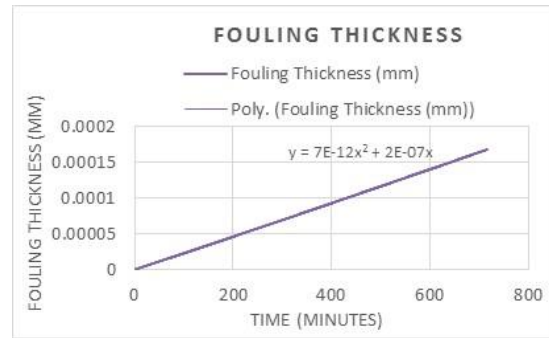
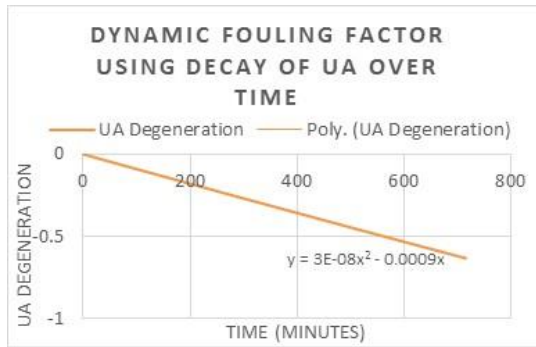


Figure 7: Dynamic fouling factor using heat transfer efficiency over time

Figure 8: Fouling thickness against time

Figure 9 shows the asymptotic fouling resistance over time which increases from 0 to 0.003. The gradient of the asymptotic fouling resistance is now known as well as all other parameters. The dynamic fouling factor can thus be written as:

$$R_f = \left((0.000004t) \left(1 - e^{-\frac{t}{t_c}} \right) \right) \quad (15)$$

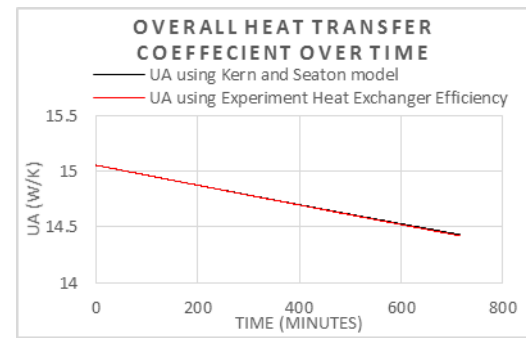
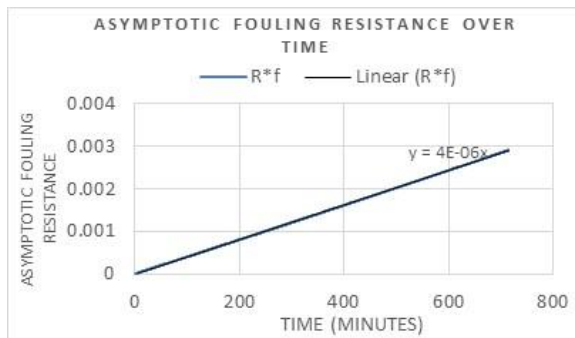


Figure 9: Asymptotic fouling resistance over time

Figure 10: Heat transfer coefficient over time

In order to validate this model, it can be compared to the model obtained from Figure 7. Eq(11) shows the fouled heat transfer coefficient obtained by comparing the clean heat transfer coefficient to the efficiency of the heat exchanger over time. Eq(5) is combined with Eq(15) and is a representation of the overall Kern and Seaton model.

$$U_f A = \frac{U_c A}{1 + U_c A \left((0.000004t) \left(1 - e^{-\frac{t}{t_c}} \right) \right)} \quad (16)$$

Figure 10 shows that the Kern and Seaton model that has been developed is comparable to the model obtained based on the heat exchanger efficiency. This shows the Kern and Seaton model can be used for this work as it matches the fouling model obtained from the experiment to a high degree of accuracy. The derivation of the dynamic heat transfer coefficient has been completed and the model can now fully operate.

4. Results and Discussion

Figures 2 and 3 show the predicted and experimental outlet temperatures for the cold stream and hot stream respectively showing some degree of discrepancy between the predicted and experimental data. Outlet stream temperatures were calculated using the E-NTU method. The hot stream temperature is over-predicted but the error is smaller as the temperature was maintained in the hot water bath better than the cold bath. This is seen in the experiment at around 400 min where the cold water temperature increases by 0.5 °C. On the other hand, the cold stream temperatures are under-predicted by around 1.5 °C throughout the experiment. Other factors that may have affected the results include the fact that the system was not well insulated which

lead to heat loss to the surroundings and that the flowrate of the hot and cold flows may not have always been exactly 1 L/min. The experiment itself should have been continued if time restrictions did not apply in order to remove significant data artefacts.

5. Conclusions

Modelling of heat exchanger fouling remains a difficult field of study and fouling remains a burden in industrial operations. Although several mathematical models have been proposed to explain the fouling behaviour of various fluids, an all-encompassing model has not emerged due to the complexity of fouling mechanism and its dependency on various operating parameters. This research has focused on a particular fouling problem when a heated saline stream has a cooling requirement. Due to the nature of the experimental equipment, low flow rates were used in order to keep the system running at steady state temperature-wise and allow adequate fouling to occur. It was found that running the experiment at high flow rates led to unstable cold stream temperatures as the residence time in the cold bath was too low to facilitate adequate cooling of the coolant stream. The aim of this work was to develop a dynamic model which reasonably described the fouling behaviour of the saline stream and to validate the model using experimental data. The development of this fouling model was based on using traditional heat exchanger models and implementing a fouling factor based on the decrease in heat transfer efficiency over time, observed experimentally. The fouling behaviour could be explained by crystallisation and precipitation mechanisms. The experimental data was analysed and a dynamic fouling model for heat transfer was developed from the findings.

The model has been validated by comparing the experimental temperature change against those predicted by the model. The model is able to accurately predict the temperature change with an average discrepancy of 1.6 °C and 0.4 °C for the cold stream and hot stream.

References

- Arsenyeva O.P., Tovazhnyansky L.L., Kapustenko P.O., Demirskyy O.V., 2012, Accounting for thermal resistance of cooling water fouling in plate heat exchangers. *Chemical Engineering Transactions*, 29, 1327-1332.
- Fryer P.J., 1989. The use of fouling models in the design of food process plant. *J. Soc. Dairy Technol.* 42, 23–29
- Georgiadis M.C., Rostein G.E., Macchietto S., 1998. Optimal design and operation of heat exchangers under milk fouling. *Aiche J.* 44(9), 2099-2111.
- Gnielinski V., 1975. Calculation of mean heat and mass transfer coefficients in laminar and turbulent flow individual bodies by means of a single equation. *Forschung im Ingenieurwesen* 41, p. 145-153 (In German).
- Haghshenasfard, M., Hooman K., 2015. CFD modeling of asphaltene deposition rate from crude oil, *Journal of Petroleum Science and Engineering*, 128, 24-32
- Jun S., Puri V.M., Roberts R.F., 2004. A dynamic 2D model for thermal performance of plate heat exchangers. *Trans. ASAE* 47(1), 213-222.
- Kern D.Q., Seaton R.E., 1959. A Theoretical Analysis of Thermal surface Fouling. *Brit. Chem. Eng.* 4(5), 258-262.
- Mérian T., Goddard J.M., 2012. Advances in nonfouling materials: perspectives for the food industry. *J. Agric. Food Chem.* 60, 2943-2957
- Müller-Steinhagen H., 2011, Heat Transfer Fouling: 50 Years After the Kern and Seaton Model. *Heat Transfer Engineering* 32(1), 1-13.
- Pääkkönen T.M., Ojaniemi U., Pättikangas T., Manninen M., Muurinen E., Keiski R.L., Simonson C.J., 2016, CFD modelling of CaCO₃ crystallization fouling on heat transfer surfaces, *International Journal of Heat and Mass Transfer*, 97, 618-630
- Pritchard A.M., Freyer P.J., 1988. Cleaning of Fouled Surfaces: A Discussion, in *Fouling Science and Technology*, NATO ASI Series, Series E: Applied Science, Melo, L. F., Bott, T. R. and Bernardo, C. A., Editors. 721-726
- Shirazi S., Lin C.J., Chen D., 2010. Inorganic fouling of pressure-driven membrane processes—a critical review, *Desalination* 250(1), 236-248.
- Sieder E.N., Tate G.E., 1936. Heat Transfer and Pressure Drop of Liquids in Tubes. *Industrial Engineering Chemistry*, 28, 1429.